A crack in a viscoelastic functionally graded material layer embedded between two dissimilar homogeneous viscoelastic layers – antiplane shear analysis

GLAUCIO H. PAULINO* and Z.-H. JIN
*Department of Civil and Environmental Engineering, University of Illinois at Urbana-Champaign, Newmark Laboratory, 205 North Mathews Avenue, Urbana, IL 61801, USA (*Author for correspondence: Fax: (217)265-8041; E-mail: paulino@uiuc.edu)*

Abstract. A crack in a viscoelastic functionally graded material (FGM) layer sandwiched between two dissimilar homogeneous viscoelastic layers is studied under antiplane shear conditions. The shear relaxation modulus of the FGM layer follows the power law of viscoelasticity, i.e., $\mu = \mu_0 \exp(\beta y/h)[t_0 \exp(\delta y/h)/t]^q$, where h is a scale length, and $\mu_0, t_0, \beta, \delta$ and q are material constants. Note that the FGM layer has position-dependent modulus and relaxation time. The shear relaxation functions of the two homogeneous viscoelastic layers are $\mu = \mu_1(t_1/t)^q$ for the bottom layer and $\mu = \mu_2(t_2/t)^q$ for the top layer, where μ_1 and μ_2 are material constants, and t_1 and t_2 are relaxation times. An elastic crack problem of the composite structure is first solved and the 'correspondence principle' is used to obtain stress intensity factors (SIFs) for the viscoelastic system. Formulae for SIFs and crack displacement profiles are derived. Several examples are given which include interface cracking between a viscoelastic functionally graded interlayer and a viscoelastic homogeneous material coating. Moreover, a parametric study is conducted considering various material and geometric parameters and loading conditions.

Key words: Antiplane shear, correspondence principle, fracture, functionally graded material, stress intensity factor, viscoelasticity.

1. Introduction

Functionally graded materials, or FGMs, are special composites that possess continuously graded properties with gradual change in microstructural details (e.g. composition, morphology, crystal structure) over predetermined geometrical orientations and distances (Hirai, 1996). For example, in a ceramic/metal FGM assemblage, the ceramic phase offers thermal barrier effects and protects the metal from corrosion and oxidation while the metal phase offers strength and toughness (Suresh and Mortensen, 1998; Tokita, 1999)

The initial emphasis for FGMs focused on thermal problems, e.g. thermal barrier coatings for space applications (Koizumi, 1993). Under high temperature, materials may exhibit creep and stress relaxation behavior. Viscoelasticity offers a basis for the study of phenomenological behavior of creep and stress relaxation. Another important area of application of viscoelasticity includes polymer-based FGMs (see, for example, Parameswaran and Shukla, 1998; Lambros et al., 1999; Marur and Tippur, 2000). In this paper, a crack in a viscoelastic FGM layer sandwiched between two dissimilar homogeneous viscoelastic layers is studied under antiplane shear conditions (Figure 1). *The shear relaxation function of the FGM layer follows the power law of viscoelasticity with position-dependent modulus and relaxation time, i.e.,*
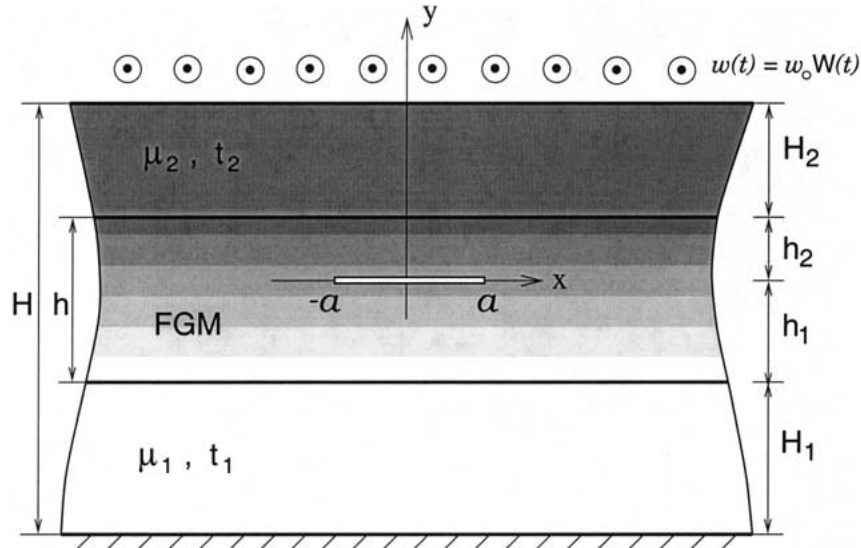
Figure 1. A viscoelastic FGM layer sandwiched between two dissimilar homogeneous viscoelastic layers occupying the region $|x| < \infty$ and $-H_1 - h_1 \le y \le H_2 + h_2$ with a crack at $|x| \le a$ and $y = 0$. The lower boundary ($y = -H_1 - h_1$) is fixed and the upper boundary ($y = H_2 + h_2$) is subjected to the uniform antiplane displacement $w_0 W(t)$.

$$\mu = \mu(y, t) = \mu_0 \exp(\beta y / h)[t_0 \exp(\delta y / h)/t]^q,$$

where h is a scale length, and $\mu_0, t_0, \beta, \delta$ and q are material constants. The shear relaxation functions of the two homogeneous viscoelastic layers are assumed as

$$\mu = \mu(t) = \mu_1(t_1/t)^q : \text{ bottom layer} \quad \text{and} \quad \mu = \mu(t) = \mu_2(t_2/t)^q : \text{ top layer},$$

where μ_1 and μ_2 are material constants, and t_1 and t_2 are relaxation times. It is noted that the FGM layer has position-dependent relaxation time, i.e. *the relaxation time of the FGM depends on the y coordinate exponentially.* An elastic crack problem of the composite structure is first solved and the 'correspondence principle' is used to obtain stress intensity factors (SIFs) for the viscoelastic system.

The antiplane shear crack problem has been extensively studied in the literature as it provides the basis for understanding the opening mode crack problem. Several numerical and analytical/semi-analytical solutions have been presented considering homogeneous materials (e.g., Paulino et al., 1993), nonhomogeneous materials (e.g., Erdogan, 1985), functionally graded coatings (e.g., Jin and Batra, 1996), homogeneous and nonhomogeneous materials with strain gradient effects (Paulino et al., 1998), bonded homogeneous viscoelastic layers (Atkinson and Chen, 1996), and a viscoelastic FGM strip (Paulino and Jin, 2001b). In the latter paper, various material models were investigated (e.g., linear standard solid, power law model without and with position-dependent relaxation time) and the solution of the viscoelastic problem employed Paulino and Jin's (2001a) revisited correspondence principle.

The present paper considers a crack in a viscoelastic FGM layer embedded between two dissimilar homogeneous viscoelastic layers subjected to antiplane shear loading. Although the solution technique employed here is the same as that in Paulino and Jin (2001b) (namely the integral equation method), the development of the solution procedure, the treatment of the boundary value problem, and the kernel involved are quite different. The main advantage of

the present solution is that it can be applied to various coating structures, for example, both an FGM coating on a homogeneous substrate and also a two-layer coating structure with an FGM interlayer can be regarded as special cases of the tri-layer structure of Figure 1. The crack may be located in the interior of the FGM layer, or at the interface between the FGM layer and a homogeneous layer. Hence, the present paper emphasizes engineering applications in important areas such as coating technologies as opposed to Paulino and Jin (2001b) that emphasizes theoretical aspects of fracture mechanics of viscoelastic FGMs.

A few additional comments about the related work by Atkinson and Chen (1996), who have also studied multilayer viscoelastic materials subjected to antiplane shear cracking, are in order. They deal with the problem of a crack lying in a homogeneous viscoelastic layer embedded in a different viscoelastic medium while we deal with the problem of a crack in a viscoelastic FGM layer sandwiched between two dissimilar homogeneous viscoelastic layers. They use the standard linear solid model, while we use the power law material model and extend such model to FGMs. They employ a free space boundary value problem where the properties of the top and bottom half space are identical, while we employ finite geometry with different properties for the top and bottom layers. Finally, we believe that our technique, using integral equation method, is simpler than the one presented by Atkinson and Chen (1996).

This manuscript is organized as follows. The next section presents the basic equations of antiplane shear for viscoelastic materials. Then, an integral equation solution approach for a crack in a viscoelastic FGM layer sandwiched between two dissimilar homogeneous viscoelastic layers is presented. Formulae for stress intensity factors (SIFs) (as a function of geometric parameters, material constants and loading) are derived considering time-dependent loading, such as exponential loading and Heaviside step function loading. Afterwards, the recovery of the displacement field is carried out and applied to obtain the actual crack profile. Numerical results for the above problem are presented and discussed. Finally, conclusions are inferred and a potential extension of this work is pointed out. An Appendix, showing the integral equation kernel derivation, supplements the paper.

2. Viscoelastic antiplane shear problem

Under antiplane shear conditions, the only nonvanishing field variables are

$$u_3(\boldsymbol{x}; t) = w(x, y; t),$$

$$\sigma_{31}(\boldsymbol{x}; t) = \tau_x(x, y; t), \quad \sigma_{32}(\boldsymbol{x}; t) = \tau_y(x, y; t),$$

$$2\varepsilon_{31}(\boldsymbol{x}; t) = \gamma_x(x, y; t), \quad 2\varepsilon_{32}(\boldsymbol{x}; t) = \gamma_y(x, y; t)$$

in which σ_{ij} are stresses, ε_{ij} are strains, t is time, and $\boldsymbol{x} = (x, y)$. The basic equations of mechanics satisfied by these variables are

$$\frac{\partial \tau_x}{\partial x} + \frac{\partial \tau_y}{\partial y} = 0, \tag{1}$$

$$\gamma_x = \frac{\partial w}{\partial x}, \quad \gamma_y = \frac{\partial w}{\partial y}, \tag{2}$$

$$\tau_x = \int_0^t \mu(x, y; t - \tau) \frac{\mathrm{d}\gamma_x}{\mathrm{d}\tau} \, \mathrm{d}\tau, \quad \tau_y = \int_0^t \mu(x, y; t - \tau) \frac{\mathrm{d}\gamma_y}{\mathrm{d}\tau} \, \mathrm{d}\tau, \tag{3}$$

where $\mu(x, y; t)$ is the shear relaxation function. *Note that for FGMs the relaxation function depends on both time and spatial position, whereas in traditional homogeneous viscoelasticity, they are only functions of time, i.e., $\mu \equiv \mu(t)$* (Christensen, 1971).

In the present study, a *power law material model* is employed. The shear relaxation modulus for the FGM is assumed as (Paulino and Jin, 2001a)

$$\mu = \mu_0 \exp(\beta \frac{y}{h}) \left[\frac{t_0 \exp(\delta y/h)}{t} \right]^q = \mu_0 \exp\left[(\beta + \delta q) \frac{y}{h} \right] \left(\frac{t_0}{t} \right)^q, \tag{4}$$

where $\mu_0, t_0, \beta, \delta, q$ are material constants and h is a scale length (see Figure 1).

3. A mode III crack in a layered FGM system

Consider an infinite viscoelastic FGM system containing a crack of length $2a$, as shown in Figure 1. The FGM layer is sandwiched between two dissimilar homogeneous viscoelastic layers. The system is fixed along the lower boundary ($y = -H_1 - h_1$) and is displaced $w(t) = w_0 W(t)$ along the upper boundary ($y = H_2 + h_2$), where w_0 is a constant, $W(t)$ is a nondimensional function of time t, H_1 and H_2 are the thicknesses of the bottom and top layers, respectively, and h_1 and h_2 (define the location of the crack) satisfy $h = h_1 + h_2$ in which h is the thickness of the FGM layer. It is assumed that the crack lies on the x-axis from $-a$ to a and is of infinite extent in the z-direction (normal to the $x - y$ plane). The crack surfaces remain traction free. The boundary conditions of the crack problem, therefore, are

$$w = 0, \quad y = -(H_1 + h_1), \ |x| < \infty, \tag{5}$$

$$w = w_0 W(t), \quad y = (H_2 + h_2), \ |x| < \infty, \tag{6}$$

$$\tau_y(x, -h_1^+) = \tau_y(x, -h_1^-), \quad |x| < \infty, \tag{7}$$

$$w(x, -h_1^+) = w(x, -h_1^-), \quad |x| < \infty, \tag{8}$$

$$\tau_y(x, h_2^+) = \tau_y(x, h_2^-), \quad |x| < \infty, \tag{9}$$

$$w(x, h_2^+) = w(x, h_2^-), \quad |x| < \infty, \tag{10}$$

$$\tau_y = 0, \quad y = 0, \ |x| \le a, \tag{11}$$

$$\tau_y(x, 0^+) = \tau_y(x, 0^-), \quad a < |x| < \infty, \tag{12}$$

$$w(x, 0^+) = w(x, 0^-), \quad a < |x| < \infty. \tag{13}$$

The shear relaxation modulus of the FGM layer is given in (4). The relaxation functions for the two homogeneous viscoelastic layers are assumed as follows

$$\mu = \mu_1 (t_1/t)^q = \mu_1 (t_1/t_0)^q (t_0/t)^q : \text{ bottom layer} \tag{14}$$

and

$$\mu = \mu_2 (t_2/t)^q = \mu_2 (t_2/t_0)^q (t_0/t)^q : \text{ top layer,} \tag{15}$$

where μ_1 and μ_2 are characteristic moduli, and t_1 and t_2 are characteristic relaxation times. To make the problem amenable to analytical treatment, the material parameter q is assumed to be the same for all the three material layers. This is a modeling restriction which implies a physical constraint in the material system.

By considering *continuity of shear relaxation modulus across the interfaces between the homogeneous layers and the FGM layer*, the constants β, δ, μ_0 and t_0 in (4) can be expressed by the material properties in the homogeneous layers as follows

$$\beta = \ln(\mu_2/\mu_1), \tag{16}$$

$$\delta = \ln(t_2/t_1), \tag{17}$$

$$\mu_0 = \mu_1(\mu_2/\mu_1)^{h_1/h}, \tag{18}$$

$$t_0 = t_1(t_2/t_1)^{h_1/h}. \tag{19}$$

According to the correspondence principle (Paulino and Jin, 2001a), one can first consider a nonhomogeneous elastic material with the following shear modulus functions

$$\mu = \mu_0 \left(\frac{\mu_1}{\mu_0}\right)\left(\frac{t_1}{t_0}\right)^q : \quad \text{bottom layer}, \tag{20}$$

$$\mu = \mu_0 \exp\left[(\beta + q\delta)\left(\frac{y}{h}\right)\right] : \quad \text{FGM layer}, \tag{21}$$

$$\mu = \mu_0 \left(\frac{\mu_2}{\mu_0}\right)\left(\frac{t_2}{t_0}\right)^q : \quad \text{top layer}. \tag{22}$$

Then the viscoelastic solution can be readily obtained by means of the correspondence principle.

For the elastic crack problem, the solution consists of a regular solution (for an uncracked strip) and a perturbed solution (by the crack). The regular stress solution can be obtained in a straightforward manner as follows

$$\tau_x = 0,$$

$$\tau_y = \tau_0 = \frac{\mu_0\tilde{\beta}w_0/h}{\exp(\tilde{\beta}h_1/h) - \exp(-\tilde{\beta}h_2/h) + (H_1/h)(\tilde{\beta}/\tilde{\mu}_1) + (H_2/h)(\tilde{\beta}/\tilde{\mu}_2)}, \tag{23}$$

where $\tilde{\beta}$, $\tilde{\mu}_1$ and $\tilde{\mu}_2$ are constants given by

$$\tilde{\beta} = \beta + q\delta, \quad \tilde{\mu}_1 = \left(\frac{\mu_1}{\mu_0}\right)\left(\frac{t_1}{t_0}\right)^q, \quad \tilde{\mu}_2 = \left(\frac{\mu_2}{\mu_0}\right)\left(\frac{t_2}{t_0}\right)^q, \tag{24}$$

respectively. The displacement in the FGM layer ($-h_1 \leq y \leq h_2$) is

$$w = \frac{w_0\left[(H_1/h)(\tilde{\beta}/\tilde{\mu}_1) + \exp(\tilde{\beta}h_1/h) - \exp(-\tilde{\beta}y/h)\right]}{\exp(\tilde{\beta}h_1/h) - \exp(-\tilde{\beta}h_2/h) + (H_1/h)(\tilde{\beta}/\tilde{\mu}_1) + (H_2/h)(\tilde{\beta}/\tilde{\mu}_2)}. \tag{25}$$

For the two homogeneous layers, the displacement for the bottom layer ($-H_1 - h_1 \leq y \leq -h_1$) is given by

$$w = \frac{w_0(\tilde{\beta}/\tilde{\mu}_1)(y + H_1 + h_1)/h}{\exp(\tilde{\beta}h_1/h) - \exp(-\tilde{\beta}h_2/h) + (H_1/h)(\tilde{\beta}/\tilde{\mu}_1) + (H_2/h)(\tilde{\beta}/\tilde{\mu}_2)} \tag{26}$$

and the displacement for the top layer ($h_2 \le y \le H_2 + h_2$) is given by

$$w = w_0 \left[1 + \frac{(\tilde{\beta}/\tilde{\mu}_2)(y - H_2 - h_2)/h}{\exp(\tilde{\beta}h_1/h) - \exp(-\tilde{\beta}h_2/h) + (H_1/h)(\tilde{\beta}/\tilde{\mu}_1) + (H_2/h)(\tilde{\beta}/\tilde{\mu}_2)} \right]. \tag{27}$$

For the perturbed problem, the following boundary conditions must be satisfied

$$w = 0, \quad y = -H_1 - h_1, \ |x| < \infty, \tag{28}$$

$$w = 0, \quad y = H_2 + h_2, \ |x| < \infty, \tag{29}$$

$$\tau_y(x, -h_1^+) = \tau_y(x, -h_1^-), \quad |x| < \infty, \tag{30}$$

$$w(x, -h_1^+) = w(x, -h_1^-), \quad |x| < \infty, \tag{31}$$

$$\tau_y(x, h_2^+) = \tau_y(x, h_2^-), \quad |x| < \infty, \tag{32}$$

$$w(x, h_2^+) = w(x, h_2^-), \quad |x| < \infty, \tag{33}$$

$$\tau_y = -\tau_0, \quad y = 0, \ |x| \le a, \tag{34}$$

$$\tau_y(x, 0^+) = \tau_y(x, 0^-), \quad a < |x| < \infty, \tag{35}$$

$$w(x, 0^+) = w(x, 0^-), \quad a < |x| < \infty, \tag{36}$$

where τ_0 is given in (23).

The displacements $w(x, y)$ are harmonic functions in the two homogeneous elastic layers, i.e.,

$$\nabla^2 w = 0, \tag{37}$$

and are governed by the following equation in the nonhomogeneous elastic (FGM) layer

$$\nabla^2 w + \frac{\tilde{\beta}}{h} \frac{\partial w}{\partial y} = 0. \tag{38}$$

By using the Fourier transform method (see, for example, Erdogan et al., 1973), the boundary value problem described by Equations (28) to (38) can be reduced to the following singular integral equation (see Appendix)

$$\int_{-1}^{1} \left[\frac{1}{s - r} + k(r, s) \right] \varphi(s) \, ds = -2\pi \frac{\tau_0}{\mu_0}, \quad |r| \le 1, \tag{39}$$

where the unknown density function $\varphi(r)$ is given by

$$\varphi(x) = \frac{\partial}{\partial x}[w(x, 0^+) - w(x, 0^-)], \tag{40}$$

the nondimensional coordinates r and s are

$$r = x/a, \quad s = x'/a, \tag{41}$$

respectively, and the Fredholm kernel $k(r, s)$ is

$$k(x, x') = a \int_0^\infty \left\{ \xi - \frac{2(m_1 A + m_2 B)(m_1 C + m_2 D)}{(m_2 - m_1)(AD - BC)} \right\} \times \frac{\sin[(x - x')\xi]}{\xi} \, \mathrm{d}\xi, \tag{42}$$

with m_1, m_2, A, B, C and D being given in the Appendix.

The function $\varphi(r)$ can be further expressed as

$$\varphi(r) = \psi(r)/\sqrt{1 - r^2}, \tag{43}$$

where $\psi(r)$ is continuous for $r \in [-1, 1]$. When $\varphi(r)$ is normalized by w_0/H, the elastic Mode III stress intensity factor (SIF), K_{III}^e, is obtained as

$$K_{III}^e = -\frac{1}{2}\mu_0 \left(\frac{w_0}{H}\right) \sqrt{\pi a} \, \psi(1). \tag{44}$$

Here, H is the total thickness of the FGM system (see Figure 1), i.e.,

$$H = H_1 + H_2 + h. \tag{45}$$

It is noted that $\psi(1)$ is dependent on several material and geometric parameters including $\mu_2/\mu_1, t_2/t_1, q, h/a, h1/h, H_1/h$ and H_2/h. Such dependencies will be investigated later in the paper (see Section 7, Results) by means of parametric studies.

4. Stress intensity factor (SIF)

The SIF for the viscoelastic FGM system can be obtained using the correspondence principle between the elastic and the Laplace transformed viscoelastic equations (Paulino and Jin, 2001a, 2001b). Thus, formulae for SIFs are derived first for exponential loading, and then the results obtained are particularized for the Heaviside step function loading.

4.1. SIF FOR EXPONENTIAL LOADING

As stated above, for nonhomogeneous viscoelastic materials, the Mode III SIF, K_{III}, can be obtained by means of the correspondence principle. The upper boundary $y = H_2 + h_2$ of the strip is subjected to a time-dependent antiplane displacement $w_0 W(t)$ as shown in Figure 1. In this case, the SIF is

$$K_{III} = -\frac{1}{2}\mu_0 \left(\frac{w_0}{H}\right) \sqrt{\pi a} \, \psi(1) \mathcal{L}^{-1} \left[t_0^q \, \Gamma(1 - q) \, p^q \, \bar{W}(p) \right], \tag{46}$$

where p is the Laplace transform variable, $\mathcal{L}^{-1}$ represents the inverse Laplace transform, $\bar{W}(p)$ is the Laplace transform of $W(t)$, and $\Gamma(\cdot)$ is the Gamma function.

Consider as an example

$$W(t) = \exp(-t/t_L) \quad \rightarrow \quad \bar{W}(p) = 1/(p + 1/t_L), \tag{47}$$

where t_L is a positive constant measuring the time variation of loads. Thus the SIF become

$$K_{III} = -\frac{1}{2}\mu_0 \left(\frac{w_0}{H}\right) \sqrt{\pi a}\ \psi(1)F(t), \tag{48}$$

where $F(t)$ is given by

$$F(t) = \left(\frac{t_0}{t}\right)^q - \frac{1}{t_L} \int_0^t \left(\frac{t_0}{\tau}\right)^q \exp\left(-\frac{t-\tau}{t_L}\right)\ d\tau. \tag{49}$$

4.2.   SIF for Heaviside step function loading

For Heaviside step loading conditions, the material system of Figure 1 is displaced w_0 along the boundary $y = H_2 + h_2$. As before, the SIF can be obtained by means of the correspondence principle, and it is given by the expression (48) with $F(t)$ being given by (cf. (49))

$$F(t) = \left(\frac{t_0}{t}\right)^q. \tag{50}$$

5.   Crack displacement profile

Accurate description of the crack profile is important in fracture mechanics, especially when the crack opening/sliding displacements are measured experimentally and correlated with numerical results. Thus the crack displacement profile for the problem illustrated in Figure 1 is recovered in this Section. First, exponential loading is considered, and then the formulation is particularized for Heaviside step function loading.

5.1.   Exponential loading

It follows from Equations (40) and (43), and the correspondence principle, that the crack sliding displacement under the time-dependent loading, $w_0 W(t)$, can be expressed by the density function $\varphi(x)$ or $\psi(r)$ (normalized by w_0/H) as follows

$$[w] = w(x,\ 0^+) - w(x,\ 0^-)$$

$$= \frac{w_0 W(t)}{H} \int_{-a}^x \varphi(x')\ dx' = w_0 W(t) \left(\frac{a}{H}\right) \int_{-1}^r \frac{\psi(s)}{\sqrt{1-s^2}}\ ds. \tag{51}$$

The displacement at the upper surface of the crack is given by

$$w(x,\ 0^+) = \frac{1}{2}[w] + \frac{1}{2\pi} \left[\frac{w_0 W(t)}{H}\right] \int_{-a}^a k_d(x,\ x')\varphi(x')\ dx'$$

$$= \frac{1}{2}[w] + \frac{w_0 W(t)}{2\pi} \left(\frac{a}{H}\right) \int_{-1}^1 k_d(r,\ s) \frac{\psi(s)}{\sqrt{1-s^2}}\ ds, \tag{52}$$

where the displacement kernel, $k_d(x,\ x')$, is

$$k_d(x, x') = -\int_0^\infty \left\{1 + \frac{2(m_1 A + m_2 B)(C + D)}{(m_2 - m_1)(AD - BC)}\right\}$$

$$\times \frac{\sin[(x-x')\xi]}{\xi}\ d\xi. \tag{53}$$

The displacement at the lower crack surface is then given by

$$w(x, \ 0^-) = w(x, \ 0^+) - [w]. \tag{54}$$

5.2. Heaviside step function loading

For Heaviside step function loading, the crack opening displacement and the displacement at the upper crack face can be obtained directly from (51) and (52) as follows

$$[w] = \ w_0 \left(\frac{a}{H}\right) \int_{-1}^{r} \frac{\psi(s)}{\sqrt{1 - s^2}} \, ds, \tag{55}$$

and

$$w(x, \ 0^+) = \frac{1}{2}[w] + \frac{w_0}{2\pi} \left(\frac{a}{H}\right) \int_{-1}^{1} k_d(r, \ s) \frac{\psi(s)}{\sqrt{1 - s^2}} \, ds, \tag{56}$$

respectively. The displacement of the lower crack face is still given by (54).

6. Numerical aspects

A comprehensive treatment of singular integral equations and their applications to crack problems can be found in the article by Erdogan et al. (1973) and the book by Hills et al. (1996). To solve the governing integral Equation (39), $\psi(r)$ is first expanded into a series of Chebyshev polynomials of the first kind. By noting the relationship (43) between $\varphi(r)$ and $\psi(r)$, the unknown $\varphi(r)$ is expressed as follows

$$\varphi(r) = \frac{\psi(r)}{\sqrt{1 - r^2}} = \frac{1}{\sqrt{1 - r^2}} \sum_{n=1}^{\infty} a_n T_n(r), \quad |r| \le 1, \tag{57}$$

where $T_n(r)$ are Chebyshev polynomials of the first kind and a_n are unknown constants. By substituting the above equation into integral Equation (58), we obtain the discrete system

$$\sum_{n=1}^{\infty} \{\pi U_{n-1}(r) + H_n(r)\} a_n = -2\pi \frac{\tau_0}{\mu_0}, \quad |r| \le 1, \tag{58}$$

where $U_{n-1}(r)$ are Chebyshev polynomials of the second kind and $H_n(r)$ are given by

$$H_n(r) = \int_{-1}^{1} ak(r, s, \beta) \frac{T_n(s)}{\sqrt{1 - s^2}} \, ds. \tag{59}$$

The detailed derivation of the governing integral equation is given in the Appendix. To solve the functional Equation (58), the series on the left side is truncated at the Nth term. A collocation technique is then used and the collocation points, r_i, are chosen as the roots of the Chebyshev polynomials of the first kind, i.e.,

$$r_i = \cos \frac{(2i - 1)\pi}{2N}, \quad i = 1, 2, \ldots, N. \tag{60}$$

The functional Equation (58) is then reduced to a linear algebraic equation system
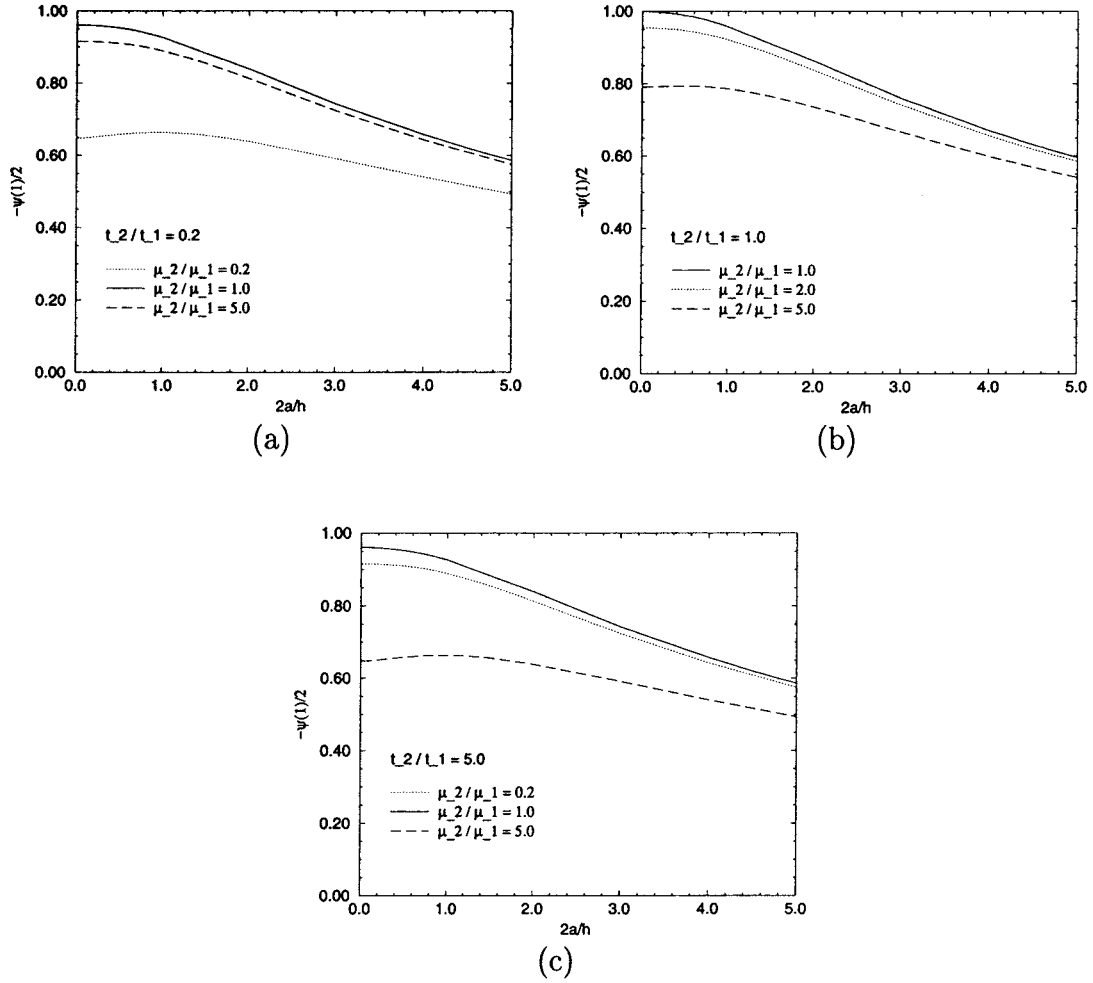
Figure 2. Normalized mode III SIF versus nondimensional crack length $2a/h$ for various shear modulus ratios μ_2/μ_1, (a) $t_2/t_1 = 0.2$; (b) $t_2/t_1 = 1.0$; (c) $t_2/t_1 = 5.0$ $(H_1 = H_2 = h, h_1 = 0.5h)$.

$$\sum_{n=1}^{N} \{\pi U_{n-1}(r_i) + H_n(r_i)\} a_n = -2\pi \frac{\tau_0}{\mu_0}, \quad i = 1, 2, \ldots, N, \tag{61}$$

where τ_0 is given by Equation (23). After $a_n(n = 1, 2, \ldots, N)$ are determined, the nondimensional SIF, $-\psi(1, \beta)/2$, is computed as follows

$$-\frac{1}{2}\psi(1, \beta) = -\frac{1}{2}\sum_{n=1}^{N} a_n. \tag{62}$$

By observing Equation (48), one verifies that the SIF is a multiplification of three parts. The first part is a dimensional base, $\mu_0(w_0/H)\sqrt{\pi a}$; the second part is a geometrical and material nonhomogeneity correction factor, $-\psi(1)/2$, which can be obtained from the numerical solution of the singular integral Equation (39); and the third part is the time evolution of SIF, $F(t)$, which is obtained (analytically) from the inverse Laplace transform.

In the following numerical calculations, 20 collocation points lead to a convergent SIF result. According to Figure 1, by taking $H_1 \rightarrow 0$, $H_2 \rightarrow 0$, and $h_1 = h_2 = h/2$ (crack located
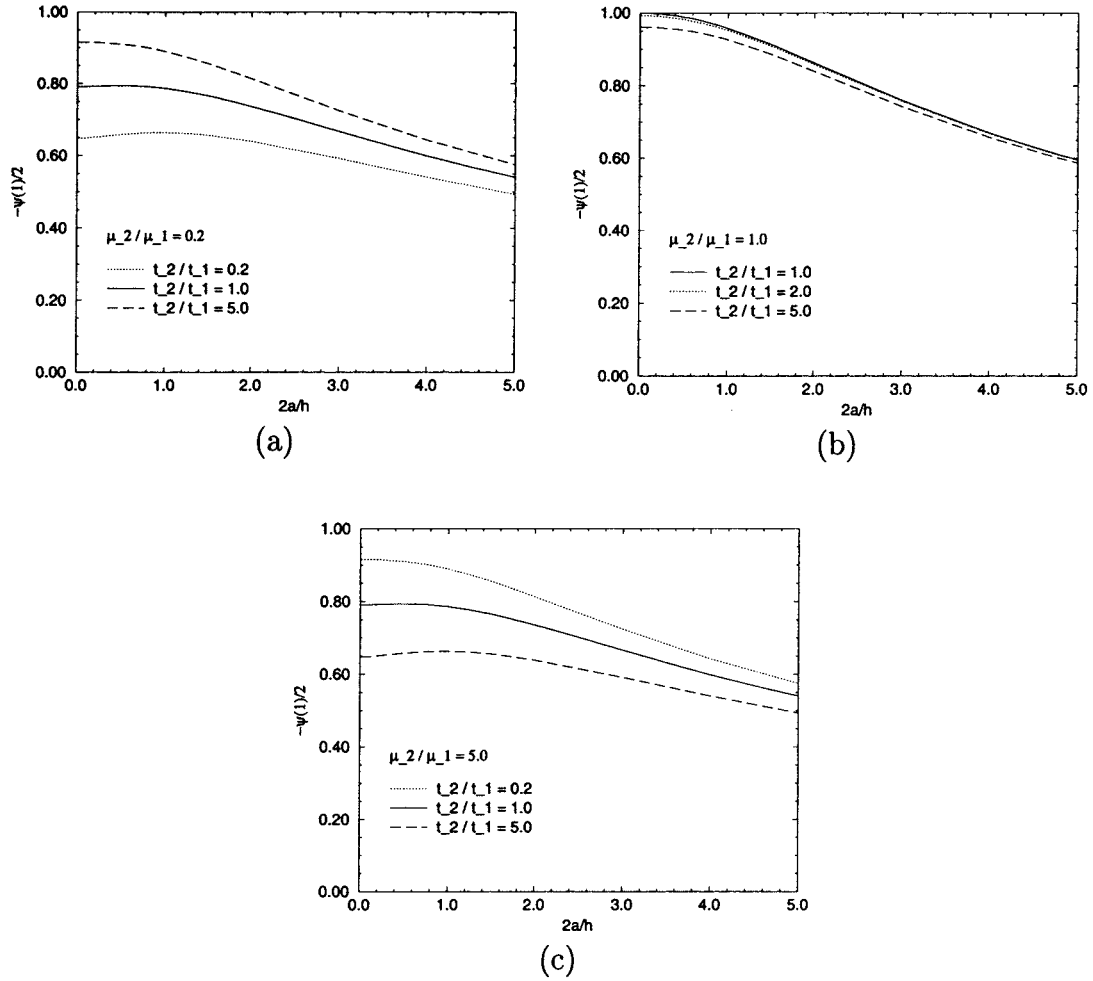
Figure 3. Normalized mode III SIF versus nondimensional crack length $2a/h$ for various relaxation time ratios t_2/t_1, (a) $\mu_2/\mu_1 = 0.2$; (b) $\mu_2/\mu_1 = 1.0$; (c) $\mu_2/\mu_1 = 5.0$ ($H_1 = H_2 = h, h_1 = 0.5h$).

at the center of the FGM layer), the single layer formulation by Paulino and Jin (2001b) is recovered as a particular case of the present formulation.

7. Results

Figures 2 and 3 show normalized SIF (see Equation (48)), $-\psi(1)/2$, versus the nondimensional crack length $2a/h$ considering various modulus ratio μ_2/μ_1 and relaxation time ratio t_2/t_1. The geometric parameters are taken as $H_1 = H_2 = h$ and $h_1 = 0.5h$, i.e., the crack is located at the center of the layered structure. The solution is valid for exponential and Heaviside step function loading (see Section 4). *In general, the normalized SIF decreases with increasing $2a/h$. This occurs because the normalization includes the parameter $1/\sqrt{a}$ in the denominator (cf., Equation (48)).* The SIF is always lower than that of the corresponding homogeneous material ($\mu_2 = \mu_1$ and $t_2 = t_1$).

Comparing the three graphs of Figure 3, one notices that the curves for the SIFs as a function of the ratio of the crack length to FGM layer thickness ($2a/h$) are further apart as
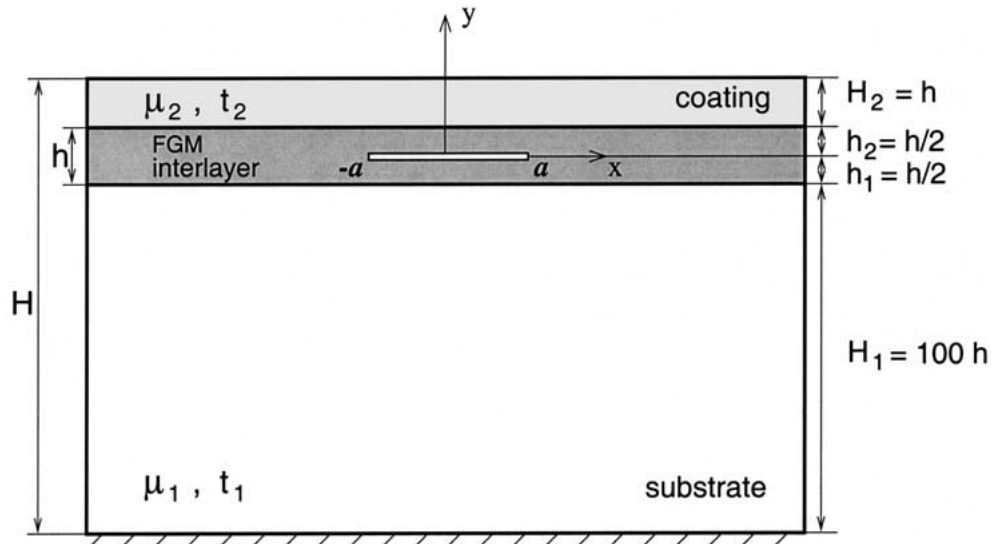
Figure 4. Coating on a substrate with an FGM interlayer. The crack is located in the middle of the FGM interlayer.

$|\mu_2/\mu_1|$ differs from 1.0. Moreover, the parameters $\mu_2/\mu_1 < 1$, $t_2/t_1 > 1$ lead to higher normalized SIFs than $t_2/t_1 < 1$ (cf., Figure 3(a)). The opposite is true when $\mu_2/\mu_1 > 1$ (cf., Figure 3(c)).

Figure 4 illustrates a coating on a substrate with an FGM interlayer. The geometric parameters are taken as $H_1 = 100h$, $H_2 = h$ and $h_1 = 0.5h$, i.e. the crack is located in the middle of the FGM layer. For this model, Figures 5 and 6 show normalized SIF, $-\psi(1)/2$, versus the nondimensional crack length $2a/h$ considering various modulus ratio μ_2/μ_1 and relaxation time ratio t_2/t_1. Comparison between Figures 2 and 5, and Figures 3 and 6, shows that the geometry has a pronounced effect on the normalized SIFs.

Figure 7 illustrates a coating on a substrate with an FGM interlayer. The geometric parameters are taken as $H_1 = 100h$, $H_2 = h$ and $h_1 = h$, i.e. the crack is located at the interface between the FGM interlayer and the coating. For this model, Figure 8 shows normalized SIF, $-\psi(1)/2$, versus the nondimensional crack length $2a/h$ considering various modulus ratio μ_2/μ_1 and a relaxation time ratio $t_2/t_1 = 1$. The overall behavior is similar to the one in Figure 5(b).

Figure 9 illustrates an FGM coating on a substrate. The geometric parameters are taken as $H_1 = 100h$, $H_2 = 0$ and $h_1 = 0.5h$, i.e. the crack is located in the middle of the FGM coating. For this model, Figure 10 shows normalized SIF, $-\psi(1)/2$, versus the nondimensional crack length $2a/h$ considering various modulus ratio μ_2/μ_1 and a relaxation time ratio $t_2/t_1 = 1$.[1] The overall behavior is similar to the ones in Figures 5(b) and 8. Thus the previous results show a significant influence of geometrical parameters (coating on a substrate versus comparable layer thickness in a tri-layer structure) on SIFs.

Figure 11 illustrates the time evolution of normalized SIF, $F(t)$, considering both exponential and Heaviside step function loading (see (49) and (50)). It is evident that under the fixed displacement condition, SIFs decrease monotonically with increasing time. By observing the

---

[1]Finite element calculations were performed for the in-plane case analogous to that of Figure 9 when $\mu_2/\mu_1 = 5.0$. The results obtained for the normalized mode I SIFs versus $2a/h$ display a flat pattern similar to that of Figure 10 (see curve for $\mu_2/\mu_1 = 5.0$).
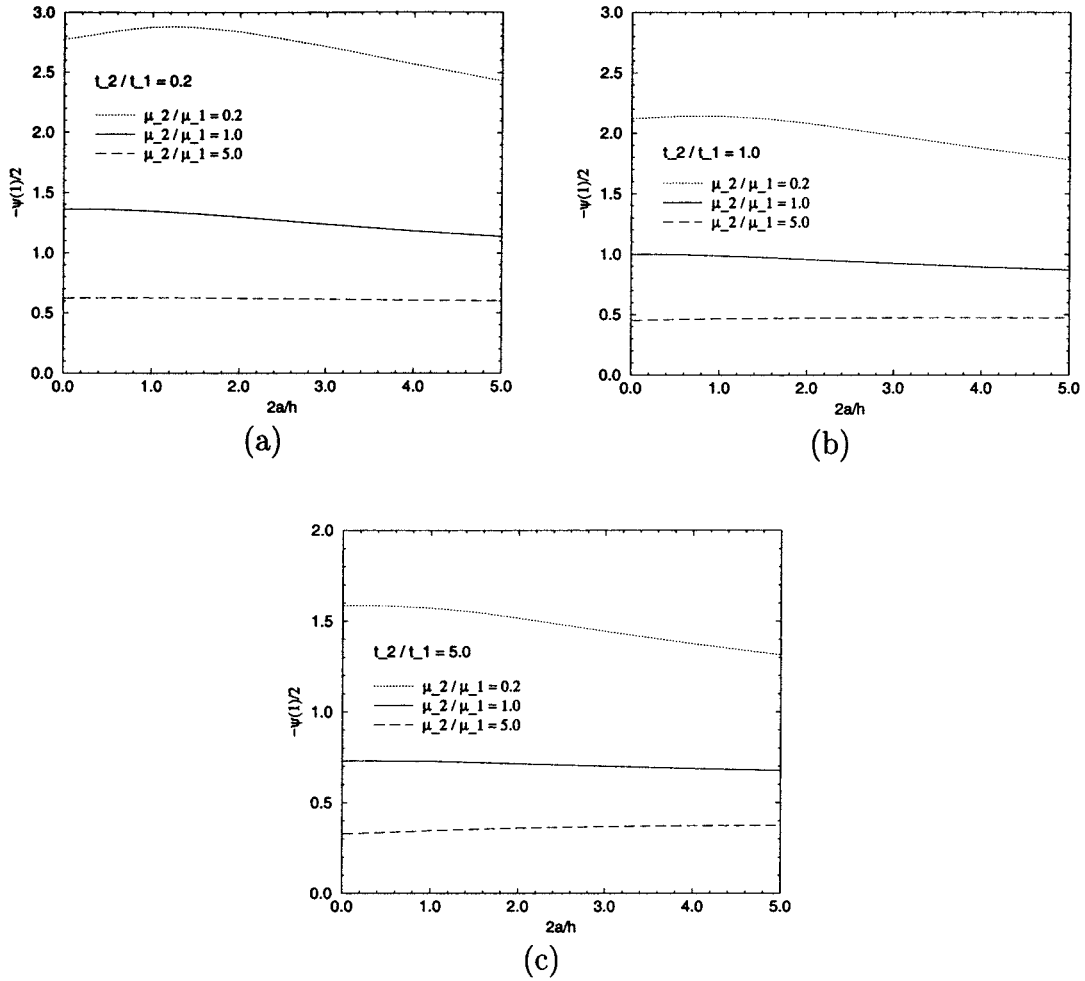
Figure 5. Normalized mode III SIF versus nondimensional crack length $2a/h$ for various shear modulus ratios μ_2/μ_1, (a) $t_2/t_1 = 0.2$; (b) $t_2/t_1 = 1.0$; (c) $t_2/t_1 = 5.0$ ($H_1 = 100h$, $H_2 = h$, $h_1 = 0.5h$) – see model in Figure 4.

plots in Figure 11, one notices that, for exponential loading, the mode III SIF can become negative as the ratio t_L/t_0 decreases, which occurs, for example, for $t_L/t_0 = 1.0$. This happens because of stress relaxation for long-time behavior.

Figure 12 illustrates the normalized SIF (normalized by $\mu_0(w_0/H)\sqrt{\pi a}$) versus time for *Heaviside step function loading* for various modulus ratio μ_2/μ_1 and a relaxation time ratio $t_2/t_1 = 1.0$. The geometric parameters are taken as $H_1 = H_2 = h$, $h_1 = 0.5h$ and $2a/h = 1.0$. The SIF decreases monotonically with increasing time. Figure 13 illustrates the normalized SIF (normalized by $\mu_0(w_0/H)\sqrt{\pi a}$) versus time for *exponential loading*. The same qualitative observations for Figure 12 also hold for Figure 13.

Figure 14 shows crack profiles for *exponential loading* for $\mu_2/\mu_1 = 5.0$, $t_2/t_1 = 1.0$, $t_L/t_0 = 5.0$ and various nondimensional times t/t_0. The geometric parameters are taken as $H_1 = H_2 = h$, $h_1 = 0.5h$ and $2a/h = 1.0$. Figure 15 shows crack profiles for *Heaviside step function loading* for relaxation time ratio $t_2/t_1 = 1.0$ and various modulus ratios μ_2/μ_1. A comparison of all the plots in Figures 14 and 15 permits to evaluate the corresponding
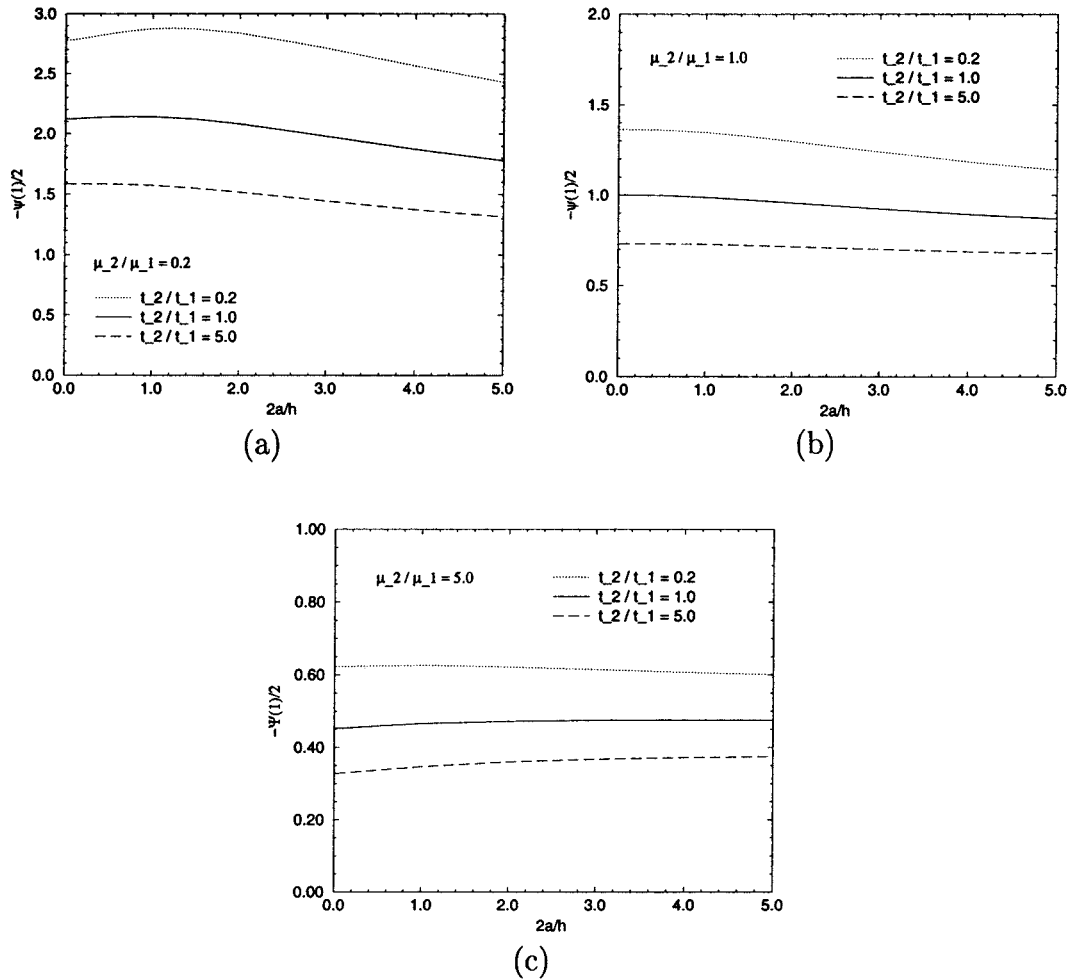
Figure 6. Normalized mode III SIF versus nondimensional crack length $2a/h$ for various relaxation time ratios t_2/t_1, (a) $\mu_2/\mu_1 = 0.2$; (b) $\mu_2/\mu_1 = 1.0$; (c) $\mu_2/\mu_1 = 5.0$ ($H_1 = 100h$, $H_2 = h$, $h_1 = 0.5h$) – see model in Figure 4.

crack profiles for various material parameters considering a representative geometry. This information is potentially valuable when correlated with fracture experiments, e.g., crack face displacement measurements.

8. Concluding remarks

This work illustrates an application of Paulino and Jin's (2001a) revisited correspondence principle to antiplane shear cracking in bonded viscoelastic layers where one of the layers is an FGM. An effective integral equation method to solve the fracture mechanics problem is presented. The elastic FGM crack problem is solved first and the correspondence principle between the elastic and the Laplace transformed viscoelastic equations is used to obtain SIFs for viscoelastic FGMs. Formulae for SIFs and crack displacement profiles are provided. Several numerical results for these quantities are presented for the power law model with both position-independent and position-dependent relaxation time. The examples emphasize
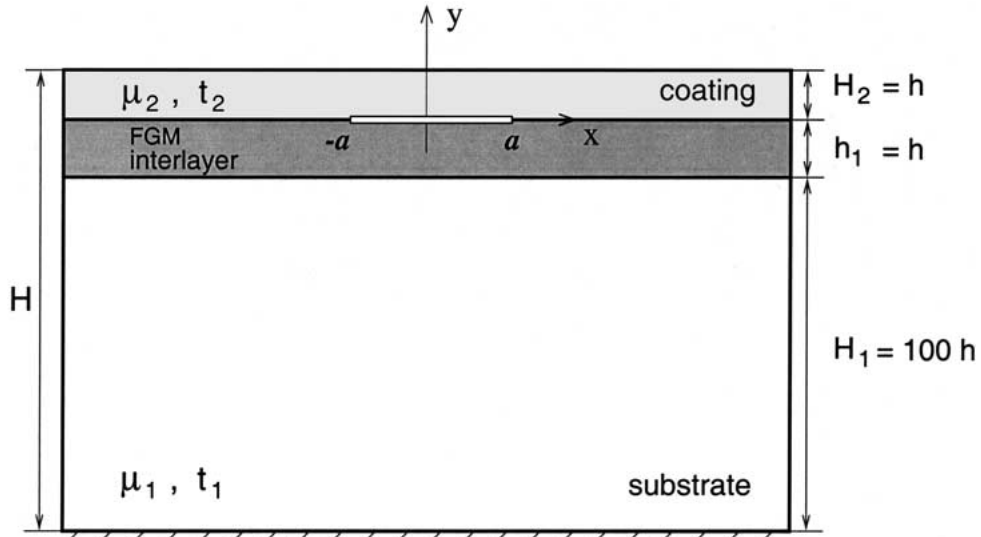
Figure 7. Coating on a substrate with an FGM interlayer. The crack is located at the interface between the top two layers.
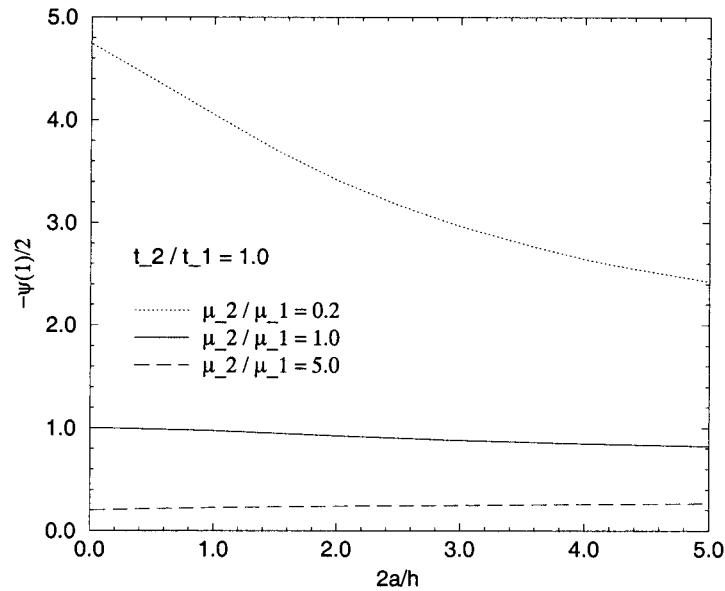
Figure 8. Normalized mode III SIF versus nondimensional crack length $2a/h$ for various shear modulus ratios $\mu_2/\mu_1, t_2/t_1 = 1.0$ ($H_1 = 100h$, $H_2 = h$, $h_1 = h$) – see model in Figure 7.

engineering applications involving coating structures with a crack located somewhere in the interior or on the boundary of the FGM (inter)layer (e.g., coating on a substrate with an FGM interlayer, FGM coating on a substrate). This investigation shows a significant influence of geometry (coating on a substrate versus comparable layer thickness in a tri-layer structure) on SIFs. This work has potential to be used to calibrate numerical methods (e.g. finite element method) for viscoelastic FGMs. Future investigation involves extension of the present investigation (on mode III crack) to mixed-mode fracture (in-plane loading). Such topic is presently being pursued by the authors.
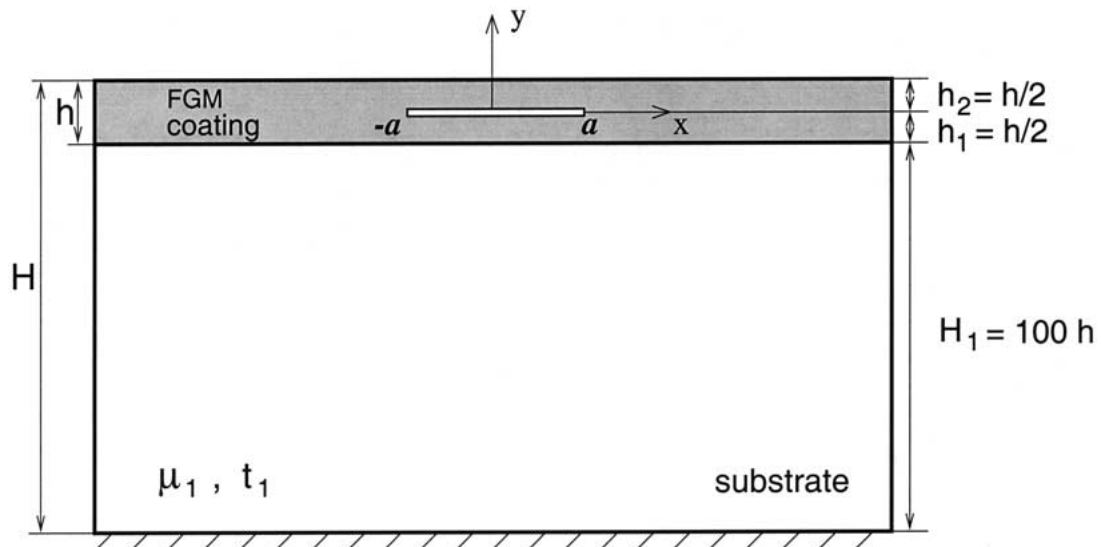
Figure 9. FGM coating on a substrate.
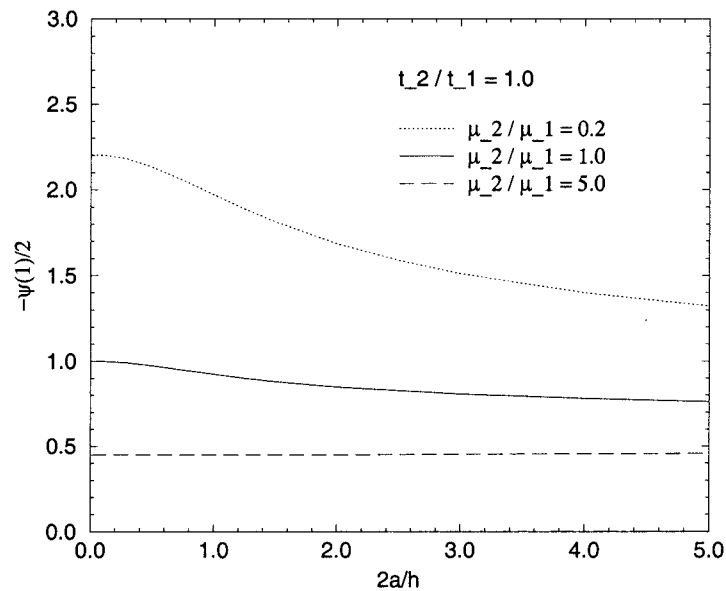
Figure 10. Normalized mode III SIF versus nondimensional crack length $2a/h$ for various shear modulus ratios μ_2/μ_1, $t_2/t_1 = 1.0$ ($H_1 = 100h$, $H_2 = 0$, $h_1 = 0.5h$) – see model in Figure 9.

Acknowledgements
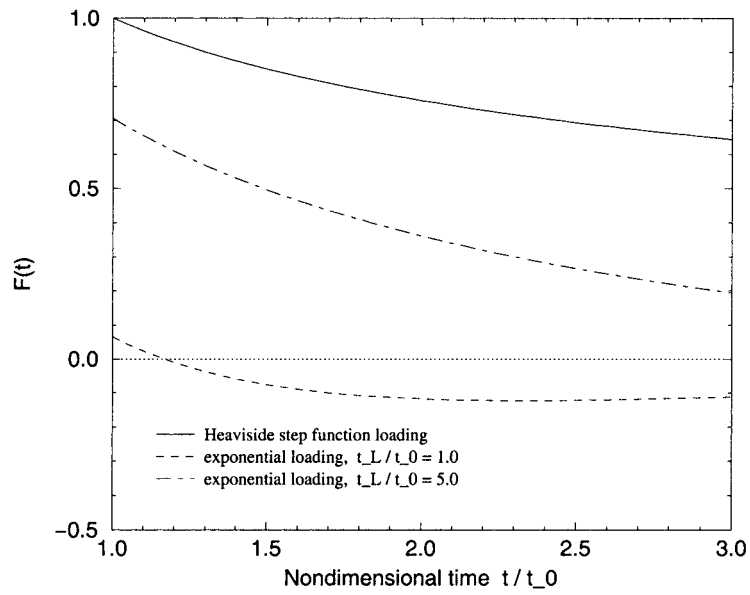
Figure 11. Time variation of normalized mode III SIF.
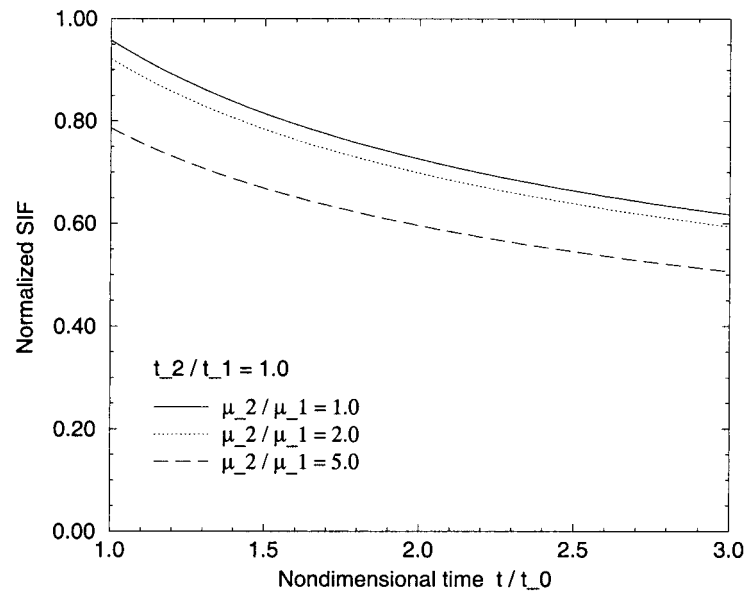
Figure 12. Normalized mode III SIF versus time: Heaviside step function loading for various modulus ratio μ_2/μ_1 ($t_2/t_1 = 1.0$, $H_1 = H_2 = h$, $h_1 = 0.5h$, $2a/h = 1.0$).

Appendix

A relatively detailed derivation of integral Equation (39) is given here, which refers to the mode III fracture mechanics problem illustrated by Figure 1. By using Fourier transform, the solution of the basic Equation (38) for the FGM layer can be expressed as
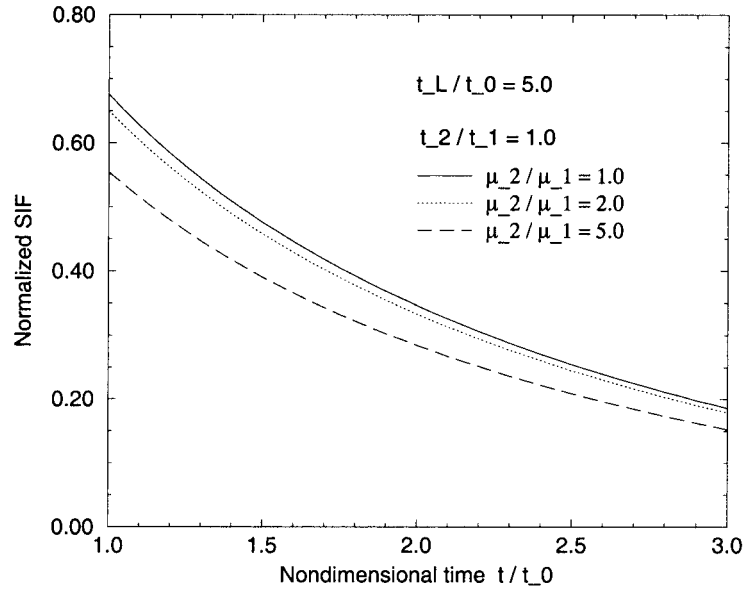
Figure 13. Normalized mode III SIF versus time: exponential loading for various modulus ratio μ_2/μ_1 ($t_L/t_0 = 5.0, t_2/t_1 = 1.0, H_1 = H_2 = h, h_1 = 0.5h, 2a/h = 1.0$).
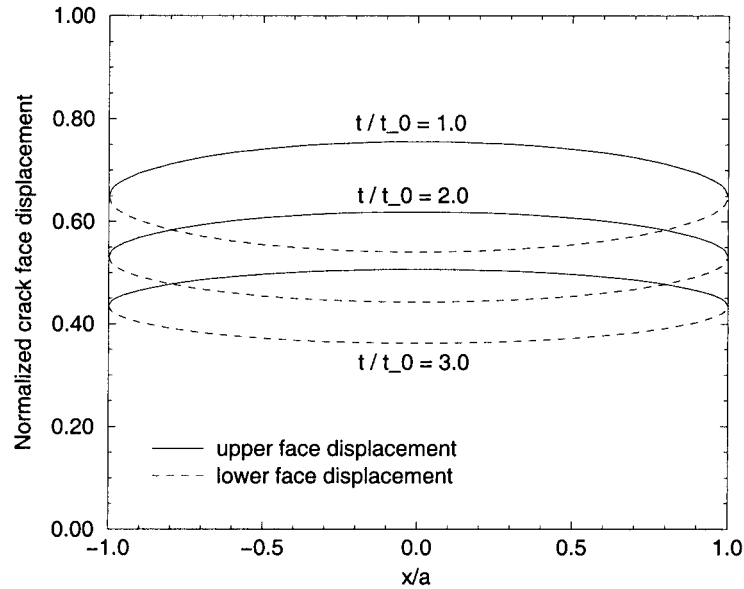
Figure 14. Crack face displacements: exponential loading ($t_L/t_0 = 5.0, \mu_2/\mu_1 = 5.0, t_2/t_1 = 1.0, H_1 = H_2 = h, h_1 = 0.5h, 2a/h = 1.0$).

$$w = \frac{1}{\sqrt{2\pi}} \int_{-\infty}^{\infty} \{A_2 \exp(m_1 y) + B_2 \exp(m_2 y)\} \exp(-ix\xi) \, \mathrm{d}\xi, \quad -h_1 \leq y \leq 0,$$

$$w = \frac{1}{\sqrt{2\pi}} \int_{-\infty}^{\infty} \{C_2 \exp(m_1 y) + D_2 \exp(m_2 y)\} \exp(-ix\xi) \, \mathrm{d}\xi, \quad 0 \leq y \leq h_2,$$

(63)

where A_2, B_2, C_2 and D_2 are unknowns, and m_1 and m_2 are given by
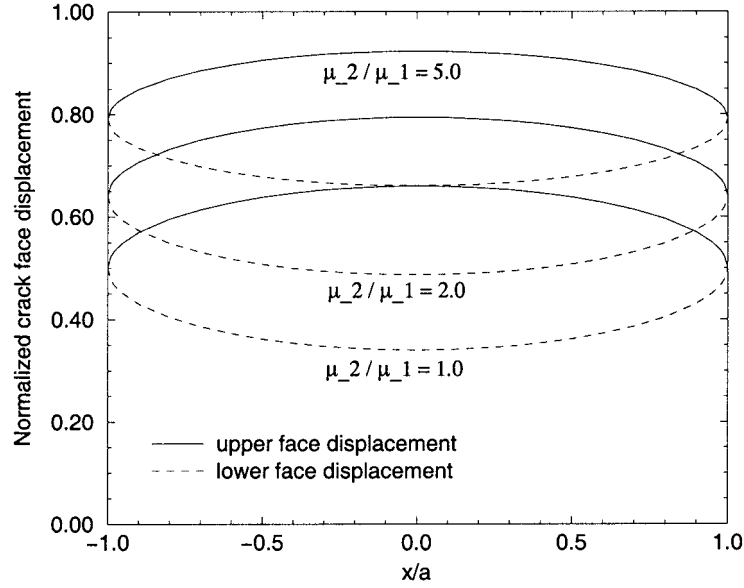
Figure 15. Crack face displacements: Heaviside step function loading for various modulus ratio μ_2/μ_1 $(t_2/t_1 = 1.0, H_1 = H_2 = h, h_1 = 0.5h, 2a/h = 1.0)$.

$$m_1 \equiv m_1(\xi) = \frac{-\tilde{\beta} + \sqrt{\tilde{\beta}^2 + 4h^2\xi^2}}{2h}, \quad m_2 \equiv m_2(\xi) = \frac{-\tilde{\beta} - \sqrt{\tilde{\beta}^2 + 4h^2\xi^2}}{2h}. \tag{64}$$

The displacements in the two homogeneous layers may be expressed as follows

$$w = \frac{1}{\sqrt{2\pi}} \int_{-\infty}^{\infty} \{A_1 \exp(-|\xi|y) + B_1 \exp(|\xi|y)\} \exp(-ix\xi)\,d\xi, \quad -H_1 - h_1 \leq y \leq -h_1,$$

$$w = \frac{1}{\sqrt{2\pi}} \int_{-\infty}^{\infty} \{A_3 \exp(-|\xi|y) + B_3 \exp(|\xi|y)\} \exp(-ix\xi)\,d\xi, \quad h_2 \leq y \leq H_2 + h_2, \tag{65}$$

where A_1, B_1, A_3 and B_3 are unknowns.

The stress τ_y is obtained from (36) and (65) through Hooke's law, i.e.

$$\tau_y = \mu_0 \exp(\tilde{\beta}y/h)\frac{\partial w}{\partial y} =$$

$$\frac{\mu_0 \exp(\tilde{\beta}y/h)}{\sqrt{2\pi}} \int_{-\infty}^{\infty} \{m_1 A_2 \exp(m_1 y) + m_2 B_2 \exp(m_2 y)\} \exp(-ix\xi)\,d\xi, \quad -h_1 \leq y \leq 0,$$

$$\tau_y = \mu_0 \exp(\tilde{\beta}y/h)\frac{\partial w}{\partial y} =$$

$$\frac{\mu_0 \exp(\tilde{\beta}y/h)}{\sqrt{2\pi}} \int_{-\infty}^{\infty} \{m_1 C_2 \exp(m_1 y) + m_2 D_2 \exp(m_2 y)\} \exp(-ix\xi)\,d\xi, \quad 0 \leq y \leq h_2,$$

$$\tau_y = \mu_0 \tilde{\mu}_1 \frac{\partial w}{\partial y} =$$

$$\frac{\mu_0 \tilde{\mu}_1}{\sqrt{2\pi}} \int_{-\infty}^{\infty} |\xi| \{-A_1 \exp(-|\xi|y) + B_1 \exp(|\xi|y)\} \exp(-ix\xi)\,d\xi, \quad -H_1 - h_1 \leq y \leq -h_1,$$

$$\tau_y = \mu_0 \tilde{\mu}_2 \frac{\partial w}{\partial y} = \tag{66}$$

$$\frac{\mu_0 \tilde{\mu}_2}{\sqrt{2\pi}} \int_{-\infty}^{\infty} |\xi| \{-A_3 \exp(-|\xi|y) + B_3 \exp(|\xi|y)\} \exp(-ix\xi) \, d\xi, \quad h_2 \leq y \leq H_2 + h_2.$$

By using the boundary conditions (28) to (36), the unknowns $A_1, A_2, B_i (i = 1, 2, 3)$ and C_2, D_2 can be expressed by A_3 which is given by

$$A_3 = -\frac{(m_1 A + m_2 B)/(i\xi\sqrt{2\pi})}{(m_2 - m_1)(AD - BC)} \int_{-a}^{a} \varphi(x') \exp(ix'\xi) \, dx', \tag{67}$$

where $\varphi(x)$ is the density function defined by (40) and A, B, C, D are known functions of ξ:

$$A = \frac{\exp[(m_1 - |\xi|)h_1]}{m_2 - m_1} \left\{ m_2[1 - \exp(-2H_1|\xi|)] - \tilde{\mu}_1|\xi| \exp(\tilde{\beta}h_1/h)[1 + \exp(-2H_1|\xi|)] \right\},$$

$$B = \frac{\exp[(m_2 - |\xi|)h_1]}{m_1 - m_2} \left\{ m_1[1 - \exp(-2H_1|\xi|)] - \tilde{\mu}_1|\xi| \exp(\tilde{\beta}h_1/h)[1 + \exp(-2H_1|\xi|)] \right\},$$

$$C = \frac{\exp[-(m_1 + |\xi|)h_2]}{m_2 - m_1} \left\{ m_2[1 - \exp(-2H_2|\xi|)] + \tilde{\mu}_2|\xi| \exp(-\tilde{\beta}h_2/h)[1 + \exp(-2H_2|\xi|)] \right\},$$

$$D = \frac{\exp[-(m_2 + |\xi|)h_2]}{m_1 - m_2} \left\{ m_1[1 - \exp(-2H_2|\xi|)] + \tilde{\mu}_2|\xi| \exp(-\tilde{\beta}h_2/h)[1 + \exp(-2H_2|\xi|)] \right\}.$$

$$\tag{68}$$

Furthermore, the stress τ_y at $y = 0$ is expressed by $\varphi(x)$ as

$$\tau_y|_{y=0} = \frac{\mu_0}{2\pi} \int_{-a}^{a} \left[\frac{1}{x' - x} + k(x, x') \right] \varphi(x') \, dx', \tag{69}$$

where $k(x, x')$ is given in (42). By substituting the above expression into the boundary condition (34), the singular integral Equation (39) is deduced.

References

Atkinson, C. and Chen, C.Y. (1996). The influence of layer thickness on the stress intensity factor of a crack lying in an elastic (viscoelastic) layer embedded in a different elastic (viscoelastic) medium (mode III analysis). *International Journal of Engineering Science* **34**, 639–658.

Christensen, R.M. (1971). *Theory of Viscoelasticity*. Academic Press, New York.

Erdogan, F. (1985). The crack problem for bonded nonhomogeneous materials under antiplane shear loading. *ASME Journal of Applied Mechanics* **52**, 823–828.

Erdogan, F., Gupta, G.D. and Cook, T.S. (1973). Numerical solution of singular integral equations. *Mechanics of Fracture*, Vol. 1 (Edited by G.C. Sih), Noordhoff, Leiden, 368–425.

Hills, D.A., Kelly, P.A., Dai, D.N. and Korsunsky, A.M. (1996). *Solution of Crack Problems: The Distributed Dislocation Technique*. Kluwer Academic Publishers, Dordrecht, The Netherlands.

Hirai, T., (1996). Functionally gradient materials. *Materials Science and Technology, 17B: Processing of Ceramics, Part 2*, (Edited by R.J. Brook), VCH Verlagsgesellschaft mbH, Weinheim, Germany, 292–341.

Jin, Z.-H. and Batra, R.C. (1996). Interface cracking between functionally graded coatings and a substrate under antiplane shear. *International Journal of Engineering Science* **34**, 1705–1716.

Koizumi, M. (1993). The concept of FGM. *Ceramic Transactions,* **34:** *Functionally Gradient Materials* (Edited by J.B. Holt, M. Koizumi, T. Hirai and Z. A. Munir), American Ceramic Society, Westerville, Ohio, 3–10.

Lambros, J. Santare, M.H., Li, H. and Sapna III, G.H. (1999). A novel technique for the fabrication of laboratory scale model functionally graded materials. *Experimental Mechanics* **39**, 183–189.

Marur P.R. and Tippur, H.V. (2000). Dynamic response of bimaterial and graded interface cracks under impact loading. *International Journal of Fracture* **103**, 95–109.

Parameswaran, V. and Shukla, A. (1998). Dynamic fracture of functionally gradient material having discrete property variation. *Journal of Material Science* **33**, 3303–3311.

Paulino, G.H., Fannjiang, A.C. and Chan, Y.S. (1999). Gradient elasticity theory for a Mode III crack in a functionally graded material. *Materials Science Forum* **308–311**, 971–976.

Paulino, G.H. and Jin, Z.-H. (2001a). Correspondence principle in viscoelastic functionally graded materials. *ASME Journal of Applied Mechanics* **68**, 129–132.

Paulino, G.H. and Jin, Z.-H. (2001b). Viscoelastic functionally graded materials subjected to antiplane shear cracking. *ASME Journal of Applied Mechanics* **68**, 284–293.

Paulino, G.H., Saif, M.T.A. and Mukherjee, S. (1993). A finite elastic body with a curved crack loaded in anti-plane shear. *International Journal of Solids and Structures* **30**, 1015–1037.

Suresh, S. and Mortensen, A. (1998) *Fundamentals of Functionally Graded Materials*. The Institute of Materials, IOM Communications Ltd., London.

Tokita, M. (1999). Development of large-size ceramic/metal bulk FGM fabricated by spark plasma sintering. *Materials Science Forum* **308–311**, 83–88.